The Mipafox-Inhibited Catalytic Domain of Human Neuropathy Target Esterase Ages by Reversible Proton Loss

ARTICLE *in* BIOCHEMISTRY · APRIL 2004

Impact Factor: 3.02 · DOI: 10.1021/bi049960e · Source: PubMed

3 AUTHORS, INCLUDING:

Rudy J Richardson
University of Michigan

123 PUBLICATIONS **3,161** CITATIONS

The Mipafox-Inhibited Catalytic Domain of Human Neuropathy Target Esterase Ages by Reversible Proton Loss†

Timothy J. Kropp,‡ Paul Glynn,§ and Rudy J. Richardson*,‡

Toxicology Program, Department of Environmental Health Sciences, University of Michigan, Ann Arbor, Michigan 48109-2029, and MRC Toxicology Unit, University of Leicester, Leicester LE1 9HN, U.K.

Received January 5, 2004; Revised Manuscript Received February 2, 2004

ABSTRACT: Aging of organophosphorus (OP)-compound-inhibited neuropathy target esterase (NTE) is the critical event that initiates OP-compound-induced delayed neurotoxicity (OPIDN). Aging has classically been considered to involve side-group loss from phosphylated NTE, rendering the enzyme refractory to reactivation. *N*,*N*′-Diisopropylphosphorodiamidofluoridate (mipafox, MIP)-inhibited NTE has been thought to age quickly; however, it can be reactivated under acidic conditions. The present study was undertaken to determine whether MIP-inhibited human recombinant NTE esterase domain (NEST) ages classically by isopropylamine loss. Diisopropylphosphorofluoridate (DFP), the oxygen analogue of MIP, was used for comparison. Kinetic values for DFP against NEST were as follows: $k_i = 17\,200 \pm 180$ M^{-1} min^{-1}; reactivation $t_{1/2} \approx 90$ min at pH 8.0 and ≈ 60 min at pH 5.2; $k_4 = 0.108 \pm 0.041$ min^{-1} at pH 8.0 and 0.181 ± 0.034 min^{-1} at pH 5.2. Kinetic values for MIP against NEST were as follows: $k_i = 1880 \pm 61$ M^{-1} min^{-1}; reactivation $t_{1/2} = 0$ min at pH 8.0 and ≈ 60 min at pH 5.2; aging was complete at all time points tested at pH 8.0, but no aging occurred at pH 5.2. Mass spectrometry revealed a mass shift of 123.0 ± 0.6 Da for the active site peptide peak of aged DFP-inhibited NEST, corresponding to a monoisopropyl phosphate adduct. In contrast, the analogous mass shift for aged MIP-inhibited NEST was 162.8 ± 0.6 Da, corresponding to the intact *N*,*N*′-diisopropylphosphorodiamido adduct. Thus, MIP-inhibited NEST does not age by isopropylamine loss. However, because kinetically aged MIP-inhibited NEST yields an intact adduct capable of reversible deprotonation, aging could occur by proton loss. Indeed, MIP-inhibited NEST does not age at pH 5.2 but ages immediately and completely at pH 8.0. Therefore, we conclude that the MIP−NEST conjugate ages by deprotonation rather than classical side-group loss.

Neuropathy target esterase (NTE[1]) is a 147 kDa integral membrane protein in the central and peripheral nervous systems, lymphocytes, and platelets best characterized as the putative target for the initiation of organophosphorus (OP)-compound-induced delayed neurotoxicity (OPIDN) (*1*−*4*). The homozygous NTE knockout is embryonic-lethal, indicating that the protein is necessary for development in mice (*5*). Nevertheless, although NTE can catalyze the hydrolysis of exogenous lysophospholipids in vitro (*6*), its physiological substrate and function have not been determined.

Initiation of OPIDN requires the concerted inhibition and aging of greater than 70% of neural NTE (*7*, *8*). Inhibition of the esterase activity of NTE likely proceeds via an S_N2 attack by the active site serine (Ser^{966}) hydroxyl group on the phosphorus atom of the OP compound with subsequent displacement of a leaving group (*9*). Aging of the phosphylated enzyme also likely occurs by an S_N2 reaction at phosphorus resulting in the loss of a side-group, creating a negatively charged phosphyl moiety covalently attached to the active site serine (*10*). This charged adduct renders the inhibited enzyme intractable to reactivation, even by strong nucleophiles, for example, KF or oximes. For at least some OP compounds, for example, diisopropylphosphorofluoridate (DFP), the side-group that is lost in the aging reaction translocates to a locus on the enzyme known as site Z (*11*, *12*).

Among classes of NTE inhibitors, phosphates, phosphonates, and phosphoroamidates (aging, neuropathic compounds) initiate OPIDN, while phosphinates, sulfonates, and carbamates (nonaging, nonneuropathic compounds) cannot initiate OPIDN, even at suprathreshold levels of inhibition (*13*−*16*). In fact, inhibition of NTE by nonaging inhibitors protects against initiation of OPIDN (*14*, *17*, *18*). It is clear, therefore, that loss of the catalytic hydrolase activity of NTE alone is not sufficient for the initiation of OPIDN but that aging is also necessary.

DFP is one of the most thoroughly studied neuropathic compounds. The aging of DFP-inhibited NTE yields an anionic monosubstituted phosphyl conjugate on the active

† This material is based upon work supported in part by the U. S. Army Research Laboratory and the U. S. Army Research Office under Grant Number DAAD19-02-1-0388.

* To whom correspondence should be addressed. Toxicology Program, Department of Environmental Health Sciences, University of Michigan, 1420 Washington Heights, Ann Arbor, MI 48109-2029. Telephone: 734-936-0769. Fax: 734-763-8095. E-mail: rjrich@umich.edu.

‡ University of Michigan.

§ University of Leicester.

[1] Abbreviations: OP, organophosphorus; NTE, neuropathy target esterase; MIP, *N*,*N*′-diisopropylphosphorodiamidofluoridate, mipafox; NEST, human recombinant NTE esterase domain; DFP, diisopropylphosphorofluoridate; OPIDN, OP-compound-induced delayed neurotoxicity; DOPC, dioleoylphosphatidylcholine; AChE, acetylcholinesterase; SELDI, surface-enhanced laser desorption/ionization; TOF MS, time-of-flight mass spectrometry; MALDI, matrix-assisted laser desorption/ionization.

10.1021/bi049960e CCC: $27.50
Published on Web 03/03/2004

Scheme 1

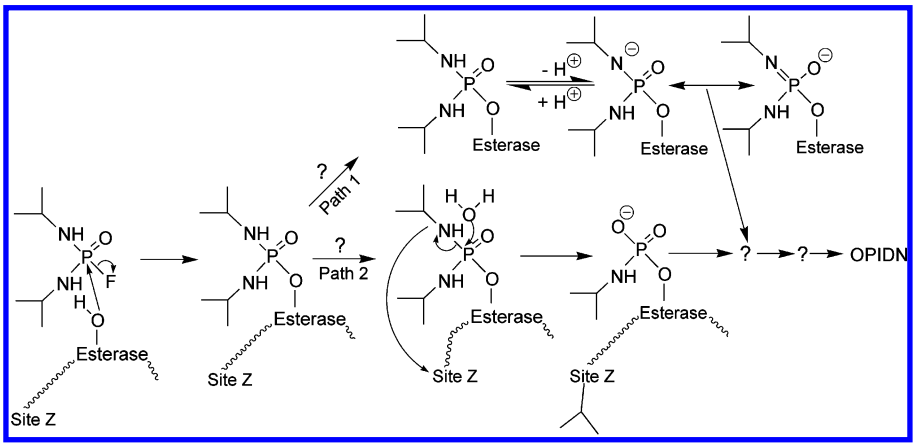

site serine of NTE (*11*, *12*, *19*). The phosphorodiamidate analogue of DFP, *N*,*N*′-diisopropylphosphorodiamidofluoridate (mipafox, MIP) produces OPIDN in vivo, just as DFP; however, the mechanism of aging is not as straightforward. Because MIP can initiate OPIDN, it has been assumed that the NTE−MIP conjugate must undergo aging (*14*, Scheme 1, path 2). The fact that NTE inhibited by MIP was initially discovered to be intractable toward reactivation strengthened this assumption (*8*). However, using standard kinetic methods, the aging of MIP-inhibited NTE was found to be complete at all time points. Consequently, it was thought that aging was too rapid to measure by these methods. Thus, the aging of MIP has not been directly demonstrated but only inferred. It has been shown more recently that KF treatment at acidic pH reactivates MIP-inhibited NTE (*20*). It was subsequently concluded that MIP-inhibited NTE had not aged as previously thought. Instead, it was suggested that the bond between the phosphoramidate and the active site serine is unusually strong. It was further speculated that the resulting perturbation in the electron distribution near the phosphoramidated serine was responsible for the stability of the complex and the onset of OPIDN.

A different interpretation of MIP-inhibited NTE is possible, however. It is known that removal of the acidic phosphoramido hydrogen on *N*-alkylphosphoramidates yields a resonance-stabilized anion (*21*). Thus, deprotonation, rather than side-group loss, provides a mechanism of aging that is plausible with respect to the data on MIP-inhibited NTE and the general knowledge of aging. However, both mechanisms share the common feature of yielding negatively charged phosphyl adducts. A deprotonation mechanism is also consistent with the fact that MIP-inhibited NTE can be reactivated at pH 5.2 but not at pH 8.0 (*22*, *23*).

Investigations of the catalytic properties of NTE in vitro have been facilitated by the availability of recombinant NTE esterase domain (NEST), comprising residues 727−1216 of human NTE (*24*). This polypeptide contains the active site serine residue, Ser^{966}, as well as two aspartates, Asp^{960} and Asp^{1086}, that are necessary for esterase activity. NEST also contains Asp^{1044} which, in possible conjunction with Asp^{1004}, is though to constitute site Z. NEST has enzymological properties similar to full-length NTE, including inactivation by OP compounds and hydrolysis of membrane lipids (*24*, *25*). In addition, it mediates an ionic conductance in liposomes that is selectively disrupted by neuropathic OP compounds (*26*). Accordingly, we used NEST in the present study to investigate questions posed about the mechanism of aging of MIP-inhibited NTE. Specifically, we tested the hypothesis that MIP-inhibited NEST ages by reversible, pH-dependent proton loss (Scheme 1, path 1) rather than classical side-group loss (Scheme 1, path 2).

MATERIALS AND METHODS

Chemicals and Enzymes. NEST was expressed, purified, and placed into dioleoylphosphatidylcholine (DOPC)-containing liposomes as described previously (*24*). Human recombinant acetylcholinesterase (AChE; EC 3.1.1.7, stock C1682, lot 062K1391) and DFP (purity by GC >99%) were purchased from Sigma (St. Louis, MO). Mipafox (purity by HPLC >99%) was purchased from ChemSyn Laboratories (Lenexa, KS). All other chemicals were the highest purity available and obtained from commercial sources.

Kinetics. Activity of the NTE-like activity of NEST in DOPC liposomes (3:1 w/w lipid/protein ratio) was determined in Tris buffer (50 mM Tris-HCl/0.20 mM EDTA, pH 8.0 at 25 °C) by a modification of the procedures described by Atkins and Glynn (*24*) and Kayyali et al. (*27*). To measure the bimolecular rate constants of inhibition (k_i), enzyme and inhibitor were incubated for various measured times. At the end of each period, substrate solution was added (phenyl valerate, final nominal concentration 2.65 mM), and incubation was carried out for a timed interval of 30−60 min. Enzyme reaction was stopped by the addition of 4-aminoantipyrine in aqueous sodium dodecyl sulfate (final concentrations 0.41 mM and 3.2 mg/mL, respectively). The chromophore was developed by addition of potassium ferricyanide (final concentration 0.06%, w/v). Absorbance was then read at 486 nm using a SPECTRAmax 340 plate reader at 25 °C (Molecular Devices Corporation, Sunnydale, CA). The k_i values for DFP and MIP against NEST were determined as previously described for other esterases (*28*−*30*).

To measure the rate constants of aging (k_4), NEST was incubated with inhibitors for 2 min at concentrations required to yield ∼90% inhibition. Reactions were performed at 25 °C in pH 8.0 and pH 5.2 Tris buffer. Aliquots of enzyme solution were then diluted 1:100 (v/v) with Tris buffer effectively to stop the inhibition reaction. The inhibited enzymes were then allowed to age for timed intervals from 0 to 18 h. At the end of each interval, an aliquot of inhibited enzyme solution was removed and incubated with KF or KCl (200 mM final concentration for each salt) for 20 min at 25

°C before determination of residual enzyme activity. In parallel, the residual activity in the absence of KF was determined to serve as a control. Reactions were performed at 25 °C. The first-order rate constants of aging (k_4) were determined as previously described for other esterases (*31*, *32*).

Mass Spectrometry. NEST was incubated in 50 mM ammonium bicarbonate buffer, pH 8.0, with concentrations of inhibitors (DFP or mipafox) determined from kinetics studies to yield greater than 90% inhibition (*32*). Additional NEST samples were also treated with KF as a fluoride control for the MIP- and DFP-treated samples or with KCl as an additional salt control. Control samples of NEST were incubated with buffer only for five sample types (MIP, DFP, KF, KCl, and no treatment). One set of samples was subjected immediately to exclusion chromatography using D-Salt Excellulose plastic desalting columns (exclusion limit, 5000 Da; Pierce Biotechnology, Rockford, IL) to remove inhibitor and subsequently subjected to tryptic digestion (see below) to attempt detection of nonaged adducts. Another set of control or inhibited samples was allowed to incubate for 0.5, 1, 2, 4, 8, 16, 24, or 168 h before inhibitor removal and tryptic digestion.

Control, inhibited, and aged samples were subjected to tryptic digestion as described by Doorn et al. (*32*). The average masses of the peptides resulting from tryptic digestion of the samples were predicted using the MS-Digest feature of ProteinProspector, version 4.0.4 (http://www.prospector.ucsf.edu/mshome4.0.htm) (*33*). Using these tools, we predicted the tryptic digest peptide containing the esterase active site serine (shown in boldface) and its associated average *m*/*z* values for the protonated molecules (MH^+) to be as follows: ALEEAGVPVDLVGGT**S**IGSFI-GALYAEER (2922.3). Adduction of the active site serine with DFP, monoisopropyl DFP, mipafox, and monoisopropyl mipafox, would result in positive average *m*/*z* shifts of 165.15, 123.07, 163.18, and 122.08, respectively.

Surface-enhanced laser desorption/ionization (SELDI) time-of-flight mass spectrometry (TOF MS) is a modification of matrix-assisted laser desorption/ionization (MALDI)-TOF MS. The SELDI or ProteinChip (Ciphergen Biosystems, Inc., Fremont, CA) technique combines MALDI-TOF MS with retentive chromatographic separation on the MALDI plate (*34*). Aliquots of nondiluted, 1:10, and 1:100 (v/v) dilutions of the peptide mixture in 50 mM ammonium bicarbonate were plated (1−3 μL) on bare gold, H4 (hydrophobic), and NP1 (hydrophilic) chips for no treatment or chromatographic treatment. No treatments on the gold chips were made. Samples for treatment were plated on H4 chips prewashed with acetonitrile (10 μL/spot) and incubated at room temperature in a humidity chamber for 20 min. The samples were then washed 3 times with 5 μL of 20% (v/v) acetonitrile per spot. Samples for treatment were also plated on NP1 chips and incubated at room temperature for 30 min in a humidity chamber. The samples were then washed twice with 2 μL of water per spot. All samples were dried at 50 °C, and 1 μL of a 50% (v/v) acetonitrile/0.5% trifluoroacetic acid (w/v) solution saturated with the matrix, α-cyano-4-hydroxycinnamic acid, was plated on top of the samples and dried at 50 °C. A PBS-II SELDI-TOF MS instrument (Ciphergen Biosystems, Inc., Fremont, CA) equipped with a nitrogen laser (337 nm, 4 ns pulse width) was used to obtain mass spectra. Analysis was carried out with an acceleration voltage of 20 kV, and 100−200 laser shots were averaged for each spectrum. The instrument was externally calibrated before each experiment in the following manner. A solution of 1 mg/mL human recombinant AChE was digested with trypsin, and the predicted peptide map was obtained as described above. Aliquots of 1 μL of AChE peptide digest were plated as described above. After drying, the sample spot was spiked with 1 μL of a 1 mg/mL dynorphin A, 1 mg/mL human angiotensin-I, 50 mM ammonium bicarbonate solution and analyzed as described above. Peptide coverage for digested AChE was 68% (data not shown). Peaks (*m*/*z*) corresponding to MH^+ AChE tryptic digest peaks, along with peaks corresponding to dynorphin A and human angiotensin-I, were used to obtain calibration for all areas in the range of the peptides obtained from digested NEST.

Table 1: Kinetic Values for MIP- and DFP-Treated NEST Samples[a]

inhibitor	k_i (M^{-1} min^{-1})	pH	k_4 (min^{-1})
MIP	1880 ± 61	8.0	*b*
		5.2	*c*
DFP	17200 ± 180	8.0	0.108 ± 0.041
		5.2	0.181 ± 0.034

[a] Values are means ± SE ($n = 4$). [b] No activity was restored for all time points (0−18 h). [c] Activity was completely restored for all time points.

RESULTS

The results of the inhibitory and postinhibitory kinetic determinations are displayed in Table 1. MIP was approximately 9 times less potent than DFP as an inhibitor of NEST. In the aging studies, no activity could be restored for MIP-inhibited NEST at pH 8.0, indicating complete and immediate aging. This apparent aging, however, could be completely restored by decreasing the pH of the system to 5.2. Activity was restored to 100% for MIP-inhibited NEST at pH 5.2 indicating that aging does not occur at this pH.

The results for the mass spectrometry experiments are contained in Table 2 and representative spectra displayed in Figure 1. All treatment-dependent mass shifts were accounted for in the MIP- and DFP-treated samples. A peak corresponding to the active site peptide adducted by a *N*,*N*′-diisopropylphosphorodiamido group was found at all time points. At no time point was a peak found corresponding to an active site peptide adducted by the *N*-monoisopropylphosphoramido moiety, indicating that classical aging does not occur. In DFP-treated NEST samples, peaks corresponding to active site peptide adducted by both intact and aged moieties were found in a time-dependent manner, as expected.

Peaks corresponding to untreated DOPC (as monomer, dimer, trimer, and tetramer with and without sodium adducts) were identified. Peaks corresponding to DOPC adducted by two fluoride ions were found in KF-treated DOPC, KF-treated NEST, and MIP- and DFP-treated NEST samples (some data not shown). Mass shifts of 37.8 ± 0.4 *m*/*z* in peaks corresponding to DOPC monomers, dimers, trimers, and tetramers were found in the KF-, MIP-, and DFP-treated NEST samples, and shifts of 37.9 ± 0.3 *m*/*z* were found in the KF-treated DOPC sample. Mass shifts of 19 *m*/*z*, corresponding to monofluoride adducts, were not found in

Table 2: MH^+ (Average Mass) for Unreacted and DFP- or MIP-Reacted NTE Active Site Peptides[a]

data type	unreacted	DFP-aged[b]	Δ*m* DFP-aged[b]	MIP-intact[c]	Δ*m* MIP-intact[c]
observed	2922.0 ± 0.2	3044.9 ± 0.2	123.0 ± 0.6	3084.8 ± 0.2	162.8 ± 0.6
theoretical	2922.3	3045.4	123.1	3085.5	163.2

[a] Mean ± SE ($n \geq 11$); all observed MH^+ showed no difference from theoretical, $p > 0.1$. [b] No peak detected corresponding to intact adduct. [c] No peak detected corresponding to classically aged adduct.

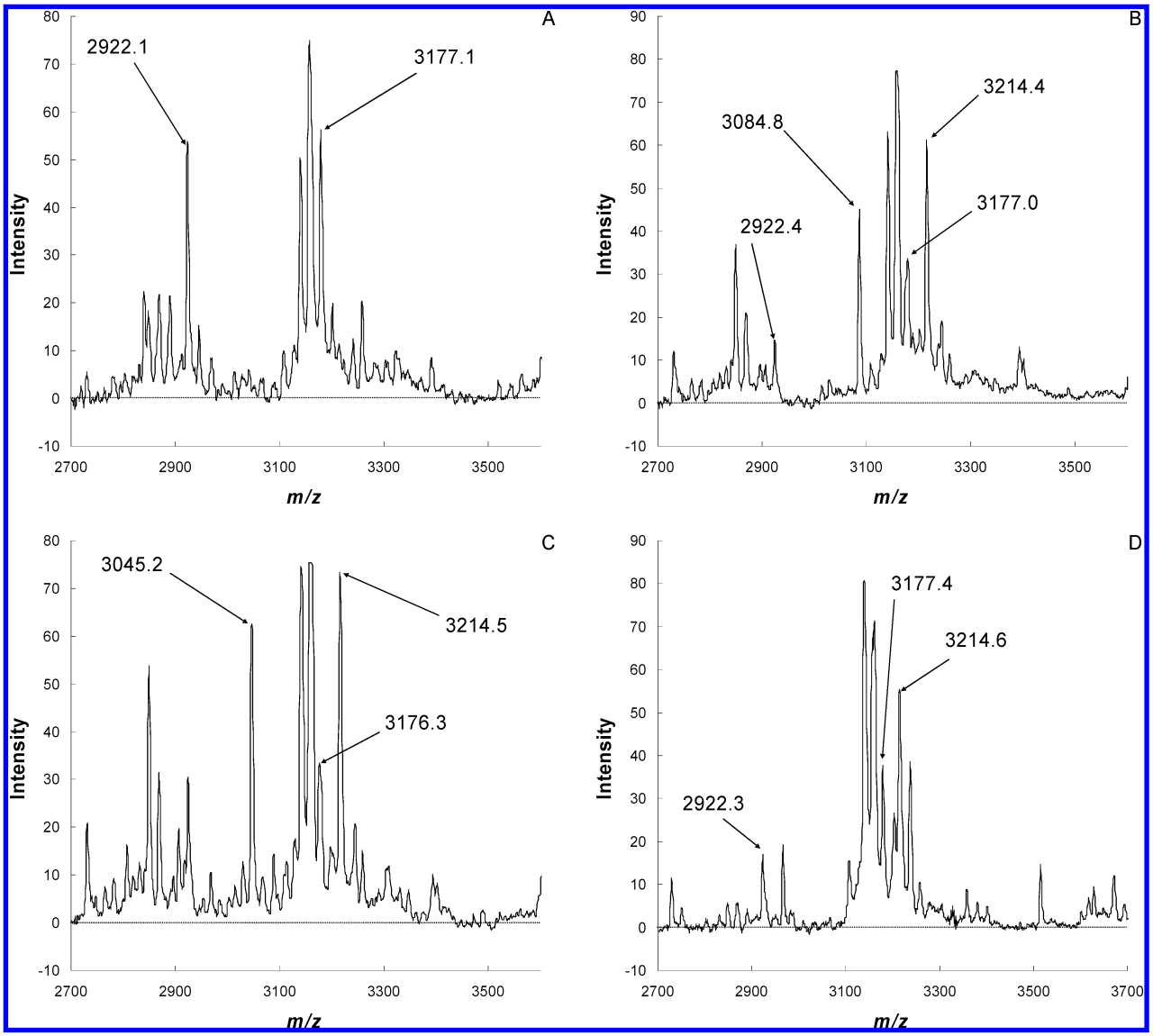

FIGURE 1: Representative SELDI-TOF MS spectra of tryptic digest of NEST samples. Panel A shows the control NEST sample. The peak with *m*/*z* of 2922.1 represents the unmodified active site peptide containing the catalytic Ser^{966}. The peak with *m*/*z* of 3177.1 represents an unmodified DOPC tetramer. Panel B shows the NEST sample modified by MIP. The peak with *m*/*z* of 3084.8 represents the active site peptide with an *N*,*N*′-diisopropylphosphorodiamido adduct. The peak with *m*/*z* of 3214.4 represents a DOPC tetramer with a difluoride adduct. Panel C shows the NEST sample modified by DFP. The peak with *m*/*z* of 3045.2 represents the active site peptide with a monoisopropyl phosphate adduct. The peak with *m*/*z* of 3214.5 represents a DOPC tetramer with a difluoride adduct. Panel D shows the NEST sample modified by KF. The peak with *m*/*z* of 3214.6 represents a DOPC tetramer with a difluoride adduct.

any of the KF-, MIP-, or DFP-treated DOPC samples. There was no difference from control for KCl-treated samples.

No mass shift was seen in peaks corresponding to likely candidate site Z peptides (*24*) (MH^+ average *m*/*z* 2586.0 and 2965.4) in either DFP- or MIP-treated samples. In DFP-treated samples, however, there was a decrease in peak intensity (signal-to-noise ratio of 12.91 to 2.32, respectively) for the peak with a MH^+ average mass of 2586.0 *m*/*z*.

Different peak coverage was found for different retentive treatments; cumulative peptide map coverage for all treatments for NEST was 74%. Sodium adducts were found in many peaks but were not found to be treatment-dependent. No treatment-dependent mass shifts were found other than those described above.

DISCUSSION

It is clear from the data presented here that MIP-inhibited NEST ages quickly at pH 8.0 and not at all at pH 5.2, supporting an aging mechanism of proton loss. This mechanism is further supported by mass spectrometry data that

show an intact *N*,*N*′-diisopropylphosphorodiamido adduct at all time points, for which kinetic methods have shown MIP-inhibited NEST to be aged. The results of this study clearly show that MIP-inhibited NEST does not age by a classical side-group loss, which would involve deletion of isopropylamine in the case of MIP-inhibited NEST (*8*, *14*). Evidence presented here leads to the conclusion that MIP-inhibited NEST ages instead by a mechanism of reversible proton loss from the *N*,*N*′-diisopropylphosphorodiamido adduct (Scheme 1, path 1). The status of the proton within the NEST enzyme system cannot be directly determined by the mass spectrometry methods employed here. Deprotonation and reprotonation may occur freely when the *N*,*N*′-diisopropylphosphorodiamido-adducted active site peptide is removed from the enzyme system by trypsinization and placed in various environments with different pH values. Nonetheless, there is high certainty that aging of MIP-inhibited NEST occurs by proton loss, because isopropylamine deletion was not found for MIP-inhibited NEST and the aging of MIP-inhibited NEST is pH-dependent and reversible. It has also been directly confirmed that DFP-inhibited NEST does age in a classical manner, corresponding to net loss of an isopropyl group as previously determined by indirect methods (*11*, *12*, *19*).

This study is the first to report k_i values for DFP or MIP against NEST. It is of interest to compare the values reported here to any previously published results for NEST. Atkins and Glynn (*24*) reported 20-min I_{50} values for MIP and DFP against NEST of $(8.7 \pm 0.2) \times 10^{-6}$ and $(9.6 \pm 0.1) \times 10^{-7}$ M, respectively, at 37 °C. The k_i values reported here for MIP and DFP against NEST correspond to 20-min I_{50} values of $(1.84 \pm 0.06) \times 10^{-5}$ and $(2.01 \pm 0.02) \times 10^{-6}$ M, respectively, using the equation $I_{50} = 0.693/(k_i t)$ (*28*, *29*). The values reported by Atkins and Glynn (*24*) differ significantly from those in the present report. However, the ratio of the values reported here to the values reported by Atkins and Glynn (*24*) are 0.88 and 0.87 for MIP and DFP, respectively. This result indicates either a real and consistent interlaboratory variation or an inherent and consistent inaccuracy of I_{50} determinations as a reflection of intrinsic inhibitory potency. In the case of DFP and MIP, however, the I_{50} determination should correlate well with the reported k_i value because the rate of spontaneous reactivation is not expected to be high. Indeed, unpublished data from this laboratory show a 20-min I_{50} for DFP against NEST of $(2.13 \pm 0.18) \times 10^{-6}$ M and× for MIP against NEST of $(1.88 \pm 0.15) \times 10^{-5}$ M, suggesting a real and consistent interlaboratory variation for absolute values. However, the data also show that ratios of 20-min I_{50} values (MIP/DFP) from each laboratory, 9.1, are the same ($p > 0.1$). Therefore, it may be more valuable to discuss relative inhibitory potencies of OP compounds against esterases using ratios rather than absolute values.

This investigation is also the first to report aging rates for DFP- or MIP-inhibited NEST. At pH 8.0, the aging of MIP-inhibited NEST was immediate (0 min) and complete, consistent with the expected rapidity of proton loss (*35*). DFP-inhibited NEST ages relatively quickly as well with $t_{1/2}$ values at pH 8.0 and 5.2 of 6.4 and 3.8 min, respectively. This aging rate is rapid compared to that of DFP-inhibited human erythrocyte AChE, which has a k_4 of 0.0025 min^{-1} ($t_{1/2} = 4.6$ h) (*28*). Previously reported values for aging of DFP-inhibited NTE include a $t_{1/2}$ value of 3−4 min (*19*) and a k_4 of 0.094 ± 0.009 min^{-1}, corresponding to a $t_{1/2}$ of 7.4 ± 0.7 min (*36*), both at pH 8.0 and 37 °C. The k_4 value reported here of 0.108 ± 0.041 min^{-1} at pH 8.0 and 25 °C corresponds to a $t_{1/2}$ of 6.42 ± 2.44 min, which is in good agreement with both previously published studies. The only other study that has reported a direct determination of MIP reactivation revealed that MIP-inhibited NTE could be fully reactivated by treatment with KF at acidic pH at 4 and 8 h (*20*). No other time points were studied; however, these data agree with the values reported here (i.e., MIP-inhibited NEST could be fully reactivated at all time points at pH 5.2).

NEST peptides have not been previously analyzed by mass spectrometry. Time-dependent aging was found for DFP-inhibited NEST using kinetics but was not found by mass spectrometry because the time for trypsinization is significantly longer than the time for DFP-inhibited NEST to age (Table 1). Both the monoisopropylphosphyl adduct found in the DFP-treated NEST sample and the diisopropylphosphyl adduct found in the MIP-treated NEST sample were determined to be extremely stable, as matching mass shifts for each species were seen in respective samples examined during the 0−168 h time course.

KF was used as a fluoride control in the mass spectrometry studies after identical MIP and DFP treatment-dependent mass shifts correlating to difluoride adducts were identified on peaks that corresponded to DOPC tetramers, trimers, dimers, and monomers. Treatment with KF resulted in similar DOPC shifts correlating to difluoride adduction (Figure 1).

Although a shift in peaks corresponding to peptides containing the proposed Z site was not found, a decrease in peak intensity was found post-DFP treatment at 2586.0 *m*/*z*, corresponding to a site Z candidate peptide (*24*). It is difficult to determine whether this decrease in intensity is an artifact related to ion suppression or due to an unknown factor. It is, however, not surprising that Z site adduction was not found; the proposed isopropyl adduct at this site is known to be unstable even within the microenvironment of the intact protein (*24*). It is possible that if an adduct were present that it was lost during trypsinization owing to its being removed from its stabilizing environment and being subjected to highly acidic conditions during preparation for analysis by mass spectrometry. It is, however, clear that no such interaction is occurring with isopropylamine after inhibition of NEST by MIP. There is no isopropylamine group loss from the NEST-MIP adduct to interact with the Z site. It is also known that MIP leads to OPIDN in vivo (*14*). These data support the hypothesis that site Z is not involved in the pathogenesis of OPIDN (*9*).

Given that the pathogenesis of OPIDN is thought to involve the creation of a negative charge in the active site of NTE (*9*) and that NEST behaves similarly to NTE (*25*), MIP-inhibited NTE also likely ages by proton loss. Future work with full-length NTE would be required to confirm this contention.

The evidence from this work and previous studies still support a mechanism of aging involving side-group loss for phosphates and phosphonates on NTE (*11*, *12*, *19*), phosphates and phosphonates on BChE (*37*, *38*), and phosphoramidates, phosphonates, and phosphates on AChE (*39*−*41*). However, the findings of the present study showing that MIP-inhibited NEST ages via deprotonation rather than side-group

loss indicate that a modification of the mechanistic definition of aging is needed. Aging has been defined operationally as a change in the inhibited enzyme that renders it intractable toward reactivation, and in this respect, the meaning of aging would not be changed. However, we now have shown that the inclusion of side-group loss in the definition would be too restrictive. A more appropriate mechanistic definition of aging would be the creation of a negative charge on the phosphyl group of the inhibited enzyme, whether this occurs by side-group loss or deprotonation.

Although recent reports have furthered knowledge about NTE (*24*−*26*, *42*), the full pathogenesis of OPIDN remains a mystery. However, the present study helps to narrow the focus for future research. It is likely that OPIDN involves disruption of a physiological function that requires inhibition and aging of NTE (*42*). Given that OP compounds that do not create a negatively charged phosphyl group are protective (*8*, *43*), it is logical to propose that the presence of this negative charge may disrupt a physiological function of NTE, which leads to axonopathy. A provocative finding in this regard is the perturbation of NEST-mediated ionic conductance across liposome membranes that occurs only when aging inhibitors of NTE and NEST are used (*6*). This is a promising avenue of research due to the differential findings for aging and nonaging compounds. However, it is still unknown whether this type of disruption would be causally related to the production of axonopathy.

In summary, the kinetic and mass spectrometry data presented here show that aging of MIP-inhibited NEST occurs by phosphoramido proton loss, not by classical side-group loss. With respect to OPIDN, these findings highlight the creation of a negative charge on the phosphyl adduct as the defining characteristic of a neuropathic compound, regardless of any interaction with site Z.

ACKNOWLEDGMENT

The authors thank Dr. Robert Christner for technical assistance and helpful discussions.

REFERENCES

1. Bertoncin, D., Russolo, A., Caroldi, S., and Lotti, M. (1985) Neuropathy target esterase in human lymphocytes, *Arch. Environ. Health 40*, 139−144.
2. Dudek, B. R., and Richardson, R. J. (1982) Evidence for the existence of neurotoxic esterase in neural and lymphatic tissue of the adult hen, *Biochem. Pharmacol. 31*, 1117−1121.
3. Maroni, M., and Bleecker, M. L. (1986) Neuropathy target esterase in human lymphocytes and platelets, *J. Appl. Toxicol. 6*, 1−7.
4. Richardson, R. J., and Dudek, B. R. (1983) Neurotoxic esterase: characterization and potential for a predictive screen for exposure to neuropathic organophosphates, in *Pesticide Chemistry: Human Welfare and the Environment* (Miyamoto, J., Kearney, P. C., Eds.) pp 491−495, Pergamon Press, Oxford. U.K.
5. Winrow, C. J., Hemming, M. L., Allen, D. M., Quistad, G. B., Casida, J. E., and Barlow, C. (2003) Loss of neuropathy target esterase in mice links organophosphate exposure to hyperactivity, *Nat. Genet. 33*, 477−485.
6. Quistad, G. B., Barlow, C., Winrow, C. J., Sparks, S. E., and Casida, J. E. (2003) Evidence that mouse brain neuropathy target esterase is a lysophospholipase, *Proc. Natl. Acad. Sci. U.S.A. 100*, 7983−7987.
7. Johnson, M. K. (1974) The primary biochemical lesion leading to the delayed neurotoxic effects of some organophosphorus esters, *J. Neurochem. 23*, 785−789.
8. Johnson, M. K. (1982) Initiation of organophosphate-induced delayed neuropathy, *Neurobehav. Toxicol. Teratol. 4*, 759−765.
9. Glynn, P. (2000) Neural development and neurodegeneration: two faces of neuropathy target esterase, *Prog. Neurobiol. 61*, 61−74.
10. Johnson, M. K. (1982) The target for initiation of delayed neurotoxicity by organophosphorus esters: biochemical studies and toxicological applications, *Rev. Biochem. Toxicol. 4*, 141−212.
11. Williams, D. G. (1983) Intramolecular group transfer is a characteristic of neurotoxic esterase and is independent of the tissue source of the enzyme. A comparison of the aging behaviour of di-isopropyl phosphorofluoridate-labeled proteins in brain, spinal cord, liver, kidney and spleen from hen and in human placenta, *Biochem. J. 209*, 817−829.
12. Williams, D. G., and Johnson, M. K. (1981) Gel-electrophoretic identification of hen brain neurotoxic esterase, labeled with tritiated di-isopropyl phosphorofluoridate, *Biochem. J. 199*, 323−333.
13. Davis, C. S., and Richardson, R. J. (1980) Organophosphorus compounds, in *Experimental and Clinical Neurotoxicology* (Spencer, P. S., Schaumburg, H. H., Eds.) pp 527−544, Williams and Wilkins, Baltimore, MD.
14. Davis, C. S., Johnson, M. K., and Richardson, R. J. (1985) Organophosphorus compounds, in *Neurotoxicity of Industrial and Commercial Chemicals* (O'Donoghue, J. L., Ed.) pp 1−23, CRC Press, Boca Raton, FL.
15. Johnson, M. K. (1975) Structure−activity relationships for substrates and inhibitors of hen brain neurotoxic esterase, *Biochem. Pharmacol. 24*, 797−805.
16. Johnson, M. K. (1970) Organophosphorus and other inhibitors of brain 'neurotoxic esterase' and the development of delayed neurotoxicity in hens, *Biochem. J. 120*, 523−531.
17. Johnson, M. K. (1990) Organophosphates and delayed neuropathy—is NTE alive and well? *Toxicol. Appl. Pharmacol. 102*, 385−399.
18. Richardson, R. J. (1984) Neurotoxic esterase: normal and pathogenic roles, in *Cellular and Molecular Neurotoxicology* (Narahashi, T., Ed.) pp 285−295, Raven Press, New York.
19. Clothier, B., and Johnson, M. K. (1979) Rapid aging of neurotoxic esterase after inhibition by di-isopropyl phosphorofluoridate, *Biochem. J. 177*, 549−558.
20. Milatović, D., and Johnson, M. K. (1993) Reactivation of phosphorodiamidated acetylcholinesterase and neuropathy target esterase by treatment of inhibited enzyme with potassium fluoride, *Chem. Biol. Interact. 87*, 425−430.
21. Eto, M. (1974) *Organophosphorus Pesticides: Organic and Biological Chemistry*, CRC Press, Cleveland, OH.
22. Richardson, R. J. (1995) Assessment of the neurotoxic potential of chlorpyrifos relative to other organophosphorus compounds: a critical review of the literature, *J. Toxicol. Environ. Health 44*, 135−165.
23. Richardson, R. J. (1998) Neurotoxicity, delayed, in *Encyclopedia of Toxicology* (Wexler, P., Ed.) pp 385−389, Academic Press, New York.
24. Atkins, J., and Glynn, P. (2000) Membrane association of and critical residues in the catalytic domain of human neuropathy target esterase, *J. Biol. Chem. 275*, 24477−24483.
25. van Tienhoven, M., Atkins, J., Li, Y., and Glynn, P. (2002) Human neuropathy target esterase catalyzes hydrolysis of membrane lipids, *J. Biol. Chem. 277*, 20942−20948.
26. Forshaw, P. J., Atkins, J., Ray, D. E., and Glynn, P. (2001) The catalytic domain of human neuropathy target esterase mediates an organophosphate-sensitive ionic conductance across liposome membranes, *J. Neurochem. 79*, 400−406.
27. Kayyali, U. S., Moore, T. B., Randall, J. C., and Richardson, R. J. (1991) Neurotoxic esterase (NTE) assay: optimized conditions based on detergent-induced shifts in the phenol/4-aminoantipyrine chromophore spectrum, *J. Anal. Toxicol. 15*, 86−89.
28. Aldridge, W. N., and Reiner, E. (1972) *Enzyme Inhibitors as Substrates: Interactions of Esterases with Esters of Organophosphorus and Carbamic Acids*, North-Holland Publishing Company, Amsterdam.
29. Richardson, R. J. (1992) Interactions of organophosphorus compounds with neurotoxic esterase, in *Organophosphates: Chemistry, Fate, and Effects* (Chambers, J. E., Levi, P. E., Eds.) pp 299−323, Academic Press, San Diego, CA.
30. Jianmongkol, S., Marable, B. R., Berkman, C. W., Tally, T. T., Thompson, C. M., and Richardson, R. J. (1999) Kinetic evidence for different mechanisms of acetylcholinesterase inhibition by (1*R*)- and (1*S*)-stereoisomers of isomalathion, *Toxicol. Appl. Pharmacol. 155*, 43−53.

31. Clothier, B., Johnson, M. K., and Reiner, E. (1981) Interaction of some trialkyl phosphorothiolates with acetylcholinesterase: characterization of inhibition, aging and reactivation, *Biochim. Biophys. Acta 660*, 306−316.
32. Doorn, J. A., Schall, M., Gage, D. A., Talley, T. T., Thompson, C. M., and Richardson, R. J. (2001) Identification of butyrylcholinesterase adducts after inhibition with isomalathion using mass spectrometry: difference in mechanism between (1R)- and (1S)-stereoisomers, *Toxicol. Appl. Pharmacol. 176*, 73−80.
33. Clauser, K. R., Baker, P. R., and Burlingame, A. L. (1999) Role of accurate mass measurement (±10 ppm) in protein identification strategies employing MS or MS/MS and database searching, *Anal. Chem. 71*, 2871−2882.
34. Issaq, H. J., Veenstra, T. D., Conrads, T. P., and Felshow, D. (2002) The SELDI-TOF MS approach to proteomics: protein profiling and biomarker identification, *Biochem. Biophys. Res. Commun. 292*, 587−592.
35. Hine, J. (1962) *Physical Organic Chemistry*, 2nd ed., pp 112−122, McGraw-Hill, New York.
36. Jokanovic, M., Stepanovic, R. M., Maksimovic, M., Kosanovic, M., and Stojiljkovic, M. P. (1998) Modification of the rate of aging of diisopropylfluorophosphate-inhibited neuropathy target esterase of hen brain, *Toxicol. Lett. 95*, 93−101.
37. Fidder, A., Hulst, A. G., Nort, D., de Ruiter, R., van der Schans, M. J., Benschop, H. P., and Langenberg, J. P. (2002) Retrospective detection of exposure to organophosphorus anti-cholinesterases: mass spectrometric analysis of phosphylated human butyrylcholinesterase, *Chem. Res. Toxicol. 15*, 582−590.
38. Masson, P., Fortier, P. L., Albaret, C., Froment, M. T., Bartels, C. F., and Lockridge, O. (1997) Aging of di-isopropyl-phosphorylated human butyrylcholinesterase, *Biochem. J. 327*, 601−607.
39. Jennings, L. L., Malecki, M., Komives, E. A., and Taylor, P. (2003) Direct analysis of the kinetic profiles of organophosphate-acetylcholinesterase adducts by MALDI-TOF mass spectrometry, *Biochemistry 42*, 11083−11091.
40. Elhanany, E., Ordentlich, A., Dgany, O., Kaplan, D., Segall, Y., Barak, R., Velan, B., and Shafferman, A. (2001) Resolving pathways of interaction of covalent inhibitors with the active site of acetylcholinesterases: MALDI-TOF/MS analysis of various nerve agent phosphyl adducts, *Chem. Res. Toxicol. 14*, 912−918.
41. Millard, C. B., Kryger, G., Ordentlich, A., Greenblatt, H. M., Harel, M., Raves, M. L., Segall, Y., Barak, D., Shafferman, A., Silman, I., and Sussman, J. L. (1999) Crystal structures of aged phosphonylated acetylcholinesterase: nerve agent reaction products at the atomic level, *Biochemistry 38*, 7032−7039.
42. Lotti, M. (1992) The Pathogenesis of organophosphate polyneuropathy, *Crit. Rev. Toxicol. 21*, 465−487.
43. Johnson, M. K., and Lauwerys, R. (1969) Protection by some carbamates against the delayed neurotoxic effects of di-isopropyl phosphorofluoridate, *Nature 222*, 1066−1067.

BI049960E